Low Reserve of Cytochrome *c* Oxidase Capacity *in Vivo* in the Respiratory Chain of a Variety of Human Cell Types*

Gaetano Villani‡§¶, Marilena Greco‡, Sergio Papa‖, and Giuseppe Attardi‡¶‖

From the ‡Division of Biology, California Institute of Technology, Pasadena, California 91125 and the ‖Institute of Medical Biochemistry and Chemistry, University of Bari, Italy

The question of whether and to what extent the *in vivo* cytochrome *c* oxidase (COX) capacity in mammalian cells exceeds that required to support respiration is still unresolved. In the present work, to address this question, a newly developed approach for measuring the rate of COX activity, either as an isolated step or as a respiratory chain-integrated step, has been applied to a variety of human cell types, including several tumor-derived semidifferentiated cell lines, as well as specialized cells removed from the organism. KCN titration assays, carried out on intact uncoupled cells, have clearly shown that the COX capacity is in low excess (16–40%) with respect to that required to support the endogenous respiration rate. Furthermore, measurements of O_2 consumption rate supported by 0.4 mM tetramethyl-*p*-phenylenediamine in antimycin-inhibited uncoupled intact cells have given results that are fully consistent with those obtained in the KCN titration experiments. Similarly, KCN titration assays on digitonin-permeabilized cells have revealed a COX capacity that is nearly limiting (7–22% excess) for ADP + glutamate/malate-dependent respiration. The present observations, therefore, substantiate the conclusion that the *in vivo* control of respiration by COX is much tighter than has been generally assumed on the basis of experiments carried out on isolated mitochondria. This conclusion has important implications for understanding the role of physiological or pathological factors in affecting the COX threshold.

In recent years, the metabolic control of oxidative phosphorylation has received growing attention, and the approach based on the "control of flux" theory (1, 2) has been increasingly applied to the study of mitochondrial metabolism since its first use for such purpose (3). The discovery that mitochondrial DNA mutations can cause diseases in humans (4, 5), affecting either components of the translation apparatus or subunits of various respiratory complexes, and the increasing evidence that a reduction in the activities of some respiratory chain complexes is associated with aging or neurodegenerative diseases have raised fundamental questions as to the degree of control that the individual steps of oxidative phosphorylation exert on the

rate of mitochondrial respiration. Most of the experimental work aimed at answering these questions has been carried out by inhibitor titration experiments on isolated mitochondria and has led to the conclusion that the activity of the various components of the respiratory chain is in excess, sometimes a large excess (2–4-fold), with evidence for a tissue-specific pattern, over the rate required to support the endogenous respiration rate (6–11). However, the issue has been recently raised as to how accurately a metabolic control analysis applied to isolated mitochondria can reflect the *in vivo* situation, considering the possible loss of essential metabolites during organelle isolation and the disruption of the normal interactions of mitochondria with the cytoskeleton, which may be important for the channeling of respiratory substrates to the organelles (12). The use of a novel approach for the analysis of overall electron flux to oxygen and of the control of respiration by cytochrome *c* oxidase (COX)[1] in intact cells has indeed revealed that the two related wild-type cell lines tested exhibited only a slightly higher COX capacity than required to support the endogenous respiration rate (12). The cells analyzed in these studies were from apparently undifferentiated established cell lines, and the tests were done after uncoupling of respiration with dinitrophenol (DNP). It therefore seemed important to apply the same type of analysis to differentiated or semidifferentiated cell types, and also to apply this analysis under more physiological conditions (state 3). This analysis has now been carried out and, as reported in the present paper, fully supports the conclusion that there is a low reserve of cytochrome *c* oxidase activity *in vivo* in the respiratory chain of a variety of human cell types.

EXPERIMENTAL PROCEDURES

Cells and Culture Conditions—The osteosarcoma-derived cell line 143B.TK⁻ (13) was grown in Dulbecco's modified Eagle's medium (DMEM) with 5% fetal bovine serum (FBS) and 100 μg/ml bromodeoxyuridine. The SKO-007 (J3) human myeloma cell line (ATCC CRL-8033–2) was grown in RPMI 1640 medium with 1 mM sodium pyruvate, 2 mM L-glutamine, 15% FBS, and 20 μg/ml 6-thioguanine. The A-549 human lung carcinoma cell line (ATCC CCL-185) was grown in DMEM with 2 mM L-glutamine and 10% FBS. The HepG2 human hepatoma cell line (ATCC HB-8065) was grown in DMEM + 10% FBS. The SH-SY5Y human neuroblastoma cell line (thrice-cloned subline of SK-N-SH (ATCC HTB11) was grown in DMEM + 15% FBS. The fibroblast strain GM056059C from the Human Genetic Mutant Cell Repository (NIGMS, National Institutes of Health), derived from a 14 month-old human male individual, was grown in DMEM with 20% FBS. Myoblast cultures derived from a normal human individual were grown in DMEM with 15% FBS. Platelets were isolated from 17 ml of blood of a rabbit by differential centrifugation and resuspended in 1.5 ml of TD (see below).

Measurement of Endogenous Respiration and DNP Titration of Endogenous Respiration in Intact Cells—Cells were collected, washed once in Tris-based, Mg^{2+}-, Ca^{2+}-deficient (TD) buffer (0.137 M NaCl, 5 mM KCl, 0.7 mM Na_2HPO_4, 25 mM Tris-HCl, pH 7.4, at 25 °C), resuspended

§ Present address: Institute of Medical Biochemistry and Chemistry, University of Bari, 70124 Bari, Italy.
¶ To whom correspondence should be addressed.

[1] The abbreviations used are: COX, cytochrome *c* oxidase; TMPD, tetramethyl-*p*-phenylenediamine; DNP, dinitrophenol; DMEM, Dulbecco's modified Eagle's medium; FBS, fetal bovine serum.

31829

Low Reserve of Cytochrome c Oxidase Capacity in Vivo

TABLE I

Effect of cell concentration in culture on endogenous respiration rate per cell

	Cell concentration in culture[a]	Endogenous O$_2$ consumption rate[b]		
		fmol of O$_2$/min/cell	nmol of O$_2$/min/mg of protein	
	cells/plate × 10^{-6}			average[c]
Osteosarcoma (143B.TK$^-$)	7.6 (6)	3.3	12.7	12.7
Myeloma (SKO-007-J3)	2.5 (2)	2.3	6.8	
	3.3 (2)	2.6	ND[d]	6.9
	4.0 (2)	1.5	7.0	
Lung carcinoma (A-549)	2.1 (2)	4.5	13.7	
	10.4 (4)	2.6	12.9	13.1
Hepatoma (Hep-G2)	3.0 (2)	13.5	17.9	
	4.4 (2)	8.6	19.2	
	6.5 (2)	6.5	ND	15.5
	9.0 (4)	6.3	12.5	
Neuroblastoma (SHSY5Y)	2.8 (2)	2.6	ND	
	6.9 (4)	1.9	8.8	8.6
	9.8 (2)	1.1	8.4	
Fibroblasts (GM05659C)	1.8 (4)	1.6	3.8	3.8

[a] Measured at time of collection. The number of determinations is indicated in parentheses.
[b] Measured in TD buffer.
[c] Average of all determinations.
[d] Not determined.

in the same buffer previously air-equilibrated at 37 °C, and transferred into a 1.5-ml water-jacketed Gilson chamber containing a small magnetic bar that was connected to a circulating water bath at 37 °C and a YS model 5300 biological oxygen monitor (Yellow Springs Instruments). After recording the endogenous respiration rate, the chamber was opened; one sample was removed for cell counting, and, in some experiments, four 20-μl samples were taken for total protein determination by the Bradford procedure (14). For DNP titration, after recording the coupled endogenous respiration rate, DNP was added at different concentrations, and the uncoupled respiratory rate was measured and expressed as percentage of the starting coupled endogenous respiration rate.

KCN Titration of COX Activity and Determination of COX$_{R(max)}$ and TMPD-supported Respiration in Intact Uncoupled Cells—The KCN titration measurements and the determination of the maximum COX capacity relative to the uninhibited endogenous respiration rate (COX$_{R(max)}$) from the threshold plots (*i.e.* the plots of relative endogenous respiration rate against percentage of inhibition of isolated COX activity at the same KCN concentrations) (7)) in DNP-uncoupled intact cells were made as described previously (12). Similarly, the measurements of the dependence on concentration of TMPD (0–2 mM), in the presence of a constant concentration of ascorbate (10 mM), of the initial O$_2$ oxygen consumption rate associated with isolated COX activity in DNP- and antimycin A-treated intact cells were carried out as detailed in the above reference.

Digitonin Titration—Cells were collected; washed once in permeabilization buffer containing 75 mM sucrose, 20 mM glucose, 5 mM KPi, 40 mM KCl, 0.5 mM EDTA, 3 mM MgCl$_2$, 30 mM Tris (pH 7.4); resuspended at 3–4 × 10^6 cells/ml in 1.5 ml of the same medium air-equilibrated at 37 °C; and supplemented with 5 units of hexokinase (type VI from bakers yeast (Sigma)) (in order to promote synthesis of glucose 6-phosphate and thus prevent accumulation of ATP) and 0.5 mM ADP, and transferred to the Gilson chamber. After recording the endogenous respiration rate, 100 nM rotenone was added to block the endogenous O$_2$ consumption, digitonin was added in different amounts from a 10% solution in dimethyl sulfoxide, and after 2 min, 5 mM succinate was added to measure the ADP-stimulated (state 3) rate of respiration of the permeabilized cells. The optimal amount of digitonin was chosen as the one giving the highest succinate-dependent respiration rate. This rate did not increase upon addition of exogenous cytochrome *c*, thus showing that the integrity of the mitochondrial outer membrane was preserved.

KCN Titration of COX Activity in Digitonin-permeabilized Cells—Samples of 143B cells, hepatoma cells and fibroblasts were collected by trypsinization and centrifugation and resuspended at about 3–4 × 10^6 cells/ml in permeabilization buffer supplemented with 1 mM phenylmethylsulfonyl fluoride, and digitonin was added at the optimal concentration (15 μg/10^6 cells for 143B cells, 10–15 μg/10^6 cells for fibroblasts (15), and 10 μg/10^6 cells for hepatoma cells). After 1–2 min, digitonin was diluted by adding 5 volumes of the same buffer containing 0.3% bovine serum albumin. The cell suspension was then centrifuged,

and the cellular pellet was resuspended at 4–6 × 10^6 cells/ml in the same buffer air-equilibrated at 37 °C and supplemented with hexokinase (5 units) and 0.5 mM ADP. In the case of 143B cells and fibroblasts, the inhibitor of adenylate kinase p1,p5-di(adenosine-5′)pentaphosphate (Ap$_5$A, Sigma) was added, at 0.15–0.3 mM, to prevent dissipation of ADP. This addition was shown, however, not to be necessary for the KCN titration measurements. Finally, two 1.5-ml portions of each cell suspension were transferred into 1.5-ml Gilson chambers attached to the same circulating water bath and the same oxygen monitor. The respiration measurements were then started by addition of 5 mM glutamate and 5 mM malate for KCN titration of the integrated COX activity, or of 20 mM antimycin A and either 10 mM ascorbate and 0.2 mM TMPD (143B cells) or 10 mM ascorbate plus 0.4 mM TMPD (hepatoma cells and fibroblasts), for KCN titration of the isolated COX activity.

In the case of the myeloma cell line, cells were collected by centrifugation, resuspended at 6–8 × 10^6 cells/ml and two 1.5-ml portions of the suspension were transferred into the Gilson chambers as described above. Digitonin was then added in the chambers at 5 μg/10^6 cells and, after 3–5 min, O$_2$ consumption measurements were started by addition of 5 mM glutamate and 5 mM malate for KCN titration of the integrated COX activity or of 20 mM antimycin A and 10 mM ascorbate and 0.4 mM TMPD for KCN titration of the isolated COX activity.

RESULTS

Cell Types Analyzed—The cells or cell derivatives chosen for analysis in the present work include several tumor-derived human cell lines, the majority of which retain some or many of the differentiated properties of the original tissue cell, such as the hepatoma HepG2 cell line (16), the lung carcinoma A-549 cell line (17), the neuroblastoma SK-N-SH cell line (18), and the SKO-007 (J3) myeloma cell line (19). Furthermore, differentiated cells removed from normal individuals (myoblasts and fibroblasts) and platelets from a rabbit were also analyzed. Therefore, the cell types investigated covered a wide range of specialized cells, and were expected to allow reasonably general conclusions about the *in vivo* control of respiration by COX.

Measurements of Coupled and Uncoupled Endogenous Respiration Rate in Intact Cells—Previous work had shown that the osteosarcoma-derived 143B.TK$^-$ cell line (13) respires in a Tris-NaCl-KCl-NaHPO$_4$ buffer (TD buffer) at the same rate as in DMEM lacking glucose (12). Table I shows the endogenous respiration rate in TD of the various cell types investigated in the present work as a function of the cell density reached by the cultures at the time of analysis. It appears that, in all cell lines analyzed, the O$_2$ consumption rate per cell tended to decrease
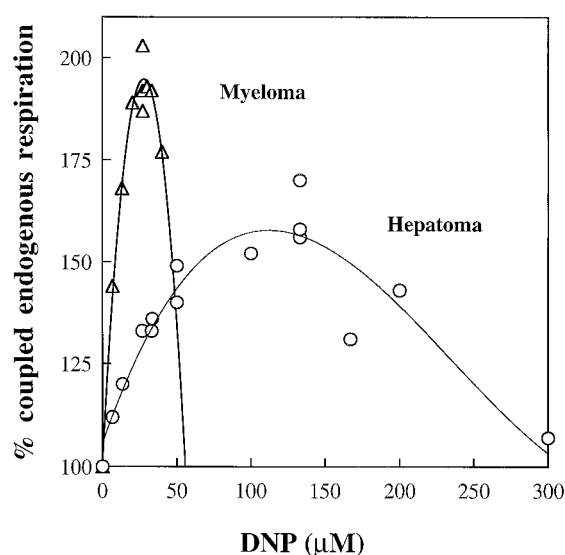
FIG. 1. **Titration of uncoupling effect of DNP.** Samples of myeloma cells ($2.7–3.3 \times 10^6$/ml) or hepatoma cells (3.3×10^6/ml) were tested for O_2 consumption rate in the presence of varying concentrations of DNP. The data are expressed relative to the coupled endogenous respiration rate set equal to 100%. Each *symbol* represents the result of a single determination.

with increasing cell density. That this decrease was due to a great extent to a decrease in size of the cells, presumably associated with an arrest of cell growth in G_1 phase, is shown by the observation that the O_2 consumption rate, normalized per mg of protein, remained constant at different densities in all cell lines, except for a slight decrease in hepatoma cells. The endogenous respiration rates per mg of protein determined in the different cell types investigated varied over a wide range, from ~3.8 nmol of O_2/min in fibroblasts to ~15.5 nmol of O_2/min in hepatoma cells.

In the present work, to exclude any effect of proton cycling and oxidative phosphorylation on the respiratory flux, the measurements were made in the presence of DNP. A titration was made of the DNP concentration that produced the highest stimulation of respiration. As exemplified in Fig. 1 for the myeloma and hepatoma cells, striking differences were observed in the titration curves obtained for the various cell types. The values obtained in different cell types for the endogenous respiration rate and for the ratio of uncoupled respiration rate, measured with the optimum DNP concentration, to coupled respiration rate (uncoupled respiration ratio) are shown in Table II. One can see that there is a large variation in uncoupled respiration ratio, ranging between 1.17 for neuroblastoma cells and 1.90 for myeloma cells. It is interesting that two normal cell types, fibroblasts and myoblasts, exhibited uncoupled respiration ratio values falling within the range observed for the various tumor-derived cell lines.

KCN Titration of COX Activity in Intact Cells—COX activity in each of the cell types investigated here was titrated, as described previously (12), with the specific inhibitor KCN both as isolated step, using 0.4 mM TMPD and 10 mM ascorbate as electron donors, in the presence of 20 nM antimycin A as upstream inhibitor, and as respiratory chain-integrated step (endogenous respiration).

As examples of the analysis performed here, Fig. 2, *a* and *c,* shows the KCN titration curves of COX activity as isolated step and as integrated step for the myeloma and hepatoma cell lines, respectively. The data are expressed as percentages of DNP-uncoupled endogenous respiration rate. The differences in the KCN titration curves of COX activity measured as isolated step and as respiratory chain-integrated step are consist-

ent with the occurrence in the myeloma and hepatoma cells of an excess of COX activity over that required to maintain a normal O_2 consumption rate, as previously observed for 143B cells (12). This excess is best illustrated by the threshold plots of Fig. 2, *b* and *d*, *i.e.* the plots of the relative endogenous respiration rate of myeloma and hepatoma cells, respectively, against the percentage of inhibition of isolated COX activity at the same KCN concentrations.

Determination of Relative Maximum COX Capacity in Intact Cells—In the plots shown in Fig. 2, *b* and *d*, if the least-square regression line through the *filled symbols* beyond the inflection point in each curve is extrapolated to zero COX inhibition, the intersection with the ordinate axis should give an estimate of the maximum COX capacity as integrated step, expressed as a percentage of the uninhibited endogenous respiration rate (see also Ref. 8). The $COX_{R(max)}$ values thus estimated for myeloma cells and hepatoma cells are ~1.33 and ~1.16, respectively. The $COX_{R(max)}$ values estimated for the different cell types investigated in this work and for the previously analyzed 143B cells (12) are shown in Table II. One can see that the excess of maximum COX capacity over the endogenous respiration rates varies between 1.16 times in hepatoma cells and 1.40 times in 143B cells, *i.e.* is much lower than previously reported for isolated rat tissue mitochondria (6, 7, 9–11). The use of the least-square regression lines through the points beyond the inflection in the threshold plots for the calculation of the COX thresholds is discussed below.

In previous work (12), the dependence on the concentration of TMPD (0–2 mM), in the presence of a constant concentration of ascorbate (10 mM), of the initial O_2 consumption rate associated with isolated COX activity was measured in DNP- and antimycin A-treated 143B cells. This analysis showed that in these cells, the uncoupled respiration rate supported by 0.4 mM TMPD, expressed relative to the uncoupled endogenous respiration rate, reached a value of 1.39, which was almost identical to the $COX_{R(max)}$ value previously determined by KCN titration for the same cells. This observation and the previous finding that, in beef heart submitochondrial particles, the steady-state level of reduction of cytochrome *c* reached a maximum at ~0.4 mM TMPD (20) suggested the possibility that measurement of the relative uncoupled respiration rate supported by 0.4 mM TMPD in DNP- and antimycin A-treated cells would provide a simplified approach for the estimation of the $COX_{R(max)}$.

Fig. 3 shows the dependence on the concentration of TMPD (from 0 to 2 mM), in the presence of a constant concentration of ascorbate (10 mM) of the COX activity, measured as an isolated step, in four of the cell types analyzed here, DNP- and antimycin A-treated (myeloma, hepatoma, lung carcinoma, and neuroblastoma). Although in all curves, as already shown for 143B cells (12), the TMPD is near-saturating above 2 mM, and starts becoming limiting at ≈0.2 mM, as previously observed for antimycin A-inhibited beef heart isolated mitochondria (21), there are some differences in the apparent saturation levels for the different cell types. The relative uncoupled respiration rates in 0.4 mM TMPD were determined for the four human cell lines analyzed in Fig. 3, as well as for human fibroblasts and myoblasts, and are shown in Table II.

One can see from Table II that the ratios of ascorbate + 0.4 mM TMPD-dependent respiration rate to endogenous respiration rate vary between 0.97 (for hepatoma cells) and 1.50 (for myoblasts). A comparison with the corresponding $COX_{R(max)}$ values determined by extrapolation of the KCN inhibition data shows a remarkable similarity between the two sets of data (within ~16%). Table II also shows the results of measurements of the ratio of ascorbate + 0.4 mM TMPD-dependent respiration rate to endogenous respiration rate in rabbit plate-

Low Reserve of Cytochrome c Oxidase Capacity in Vivo

TABLE II

Uncoupled to coupled respiration ratio (UCR), relative uncoupled respiration rate at 400 μM TMPD (AT 400/DNP end.resp.), relative COX capacity (COX$_{Rmax}$), and COX threshold (COX$_T$) in intact uncoupled cells (DNP) or in digitonin-permeabilized cells in state 3

See under "Experimental Procedures" for details.

	UCR[a]	AT 400/DNP end. resp.[b]	COX$_{R(max)}$		COX$_T$	
			(DNP) intact cells[c]	(ADP + Glu/ Mal) permeable cells[d]	(DNP) intact cells[e]	(ADP + Glu/ Mal) permeable cells[e]
143B.TK$^-$	1.35	1.39 ± 0.03	1.40	1.22	28	18
Myeloma	1.90 ± 0.03	1.14 ± 0.01	1.33	1.15	25	13
Lung carcinoma	1.32 ± 0.03	1.51 ± 0.02	1.33		25	
Hepatoma	1.65 ± 0.03	0.97 ± 0.02	1.16	1.20	14	17
Neuroblastoma	1.17 ± 0.02	1.02 ± 0.01	1.21		17	
Fibroblasts	1.44 ± 0.04	1.27 ± 0.09	1.19	1.07	16	7
Myoblasts	1.50 ± 0	1.50 ± 0.05				
Platelets (rabbit)		1.42				

[a] Data derived from two or three independent experiments (three to eight determinations) and from Villani and Attardi (12) for 143B.TK$^-$ cells. The average and S.E. are shown.

[b] Data derived from one or two independent experiments (two to four determinations, one for platelets) and from Villani and Attardi (12) for 143B.TK$^-$ cells.

[c] Data taken from experiments shown in Fig. 2, *b* and *d*, and similar experiments carried out with 143B.TK$^-$ cells (12) with lung carcinoma cells (three independent experiments, seven determinations), neuroblastoma cells (two experiments, four determinations), and fibroblasts (one determination).

[d] Data taken from experiments shown in Fig. 5 and a similar experiment carried out with fibroblasts (one determination).

[e] Data derived from the COX$_{R(max)}$ values in this table.
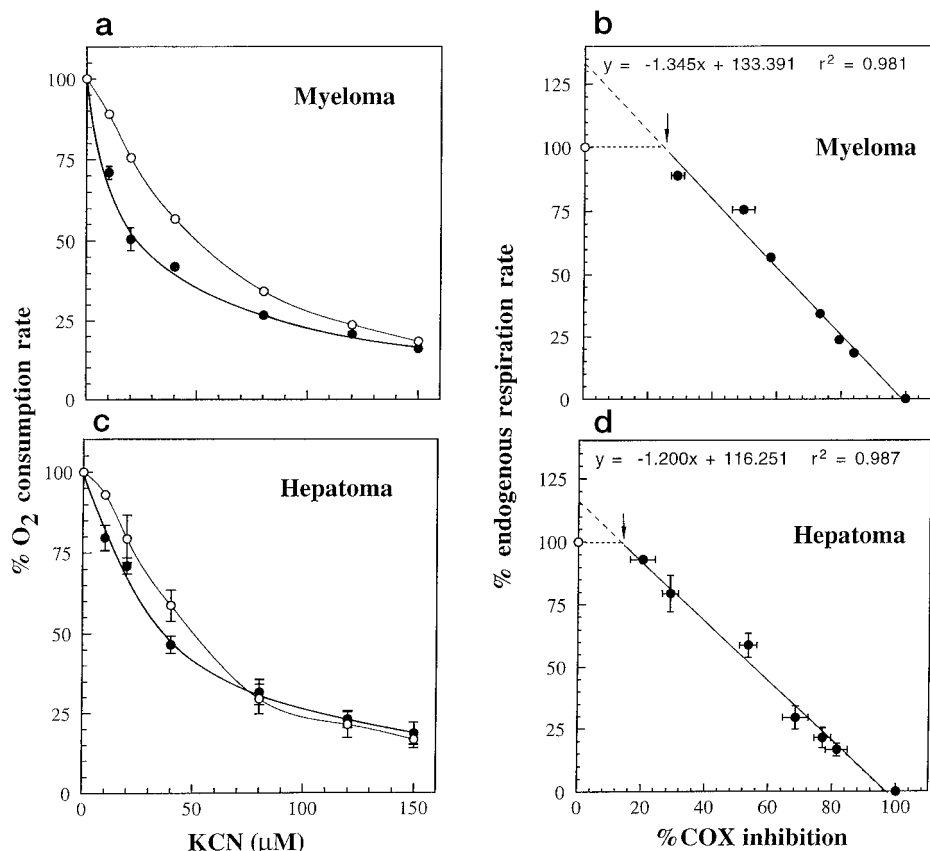

FIG. 2. **Inhibition by KCN of endogenous respiration rate in TD buffer in the presence of DNP (○) or of ascorbate + 0.4 mM TMPD-dependent respiration rate in TD buffer in the presence of DNP and antimycin A (●) in intact myeloma cells (*a*) or hepatoma cells (*c*), and percentage of endogenous respiration rate as a function of percentage of COX inhibition in myeloma cells (*b*) or hepatoma cells (*d*) with determination of maximum COX capacity (COX$_{R(max)}$).** *a* and *c*, the data of O$_2$ consumption rate shown represent the means ± S.E. (the *error bars* that fall within the individual data symbols are not shown) obtained in four determinations (three independent experiments) on myeloma cells and in seven determinations (two experiments) on hepatoma cells. The concentration of cells in the measuring chamber was 2.7–3.3 × 10^6/ml for myeloma and 3.3 × 10^6/ml for hepatoma. *b* and *d*, the percentage rates of endogenous respiration in the experiments illustrated in *a* and *c*, respectively, are plotted against percentage of COX inhibition by KCN, and the least-square regression line through the *filled symbols* beyond the inflection point in each curve (*arrow*) is extended to zero COX inhibition. The equations describing these extrapolated lines are shown.

lets, which gave a value of 1.42.

Relative COX Capacity in Human Cells in State 3—The analysis of relative COX capacity described above was carried out in uncoupled intact cells. It seemed, therefore, important to

test whether the conclusion reached about the nearly limiting or low excess of COX activity in the respiratory chain of several different human cell types also applies to cells permeabilized with digitonin and tested in state 3 respiration, *i.e.* under more
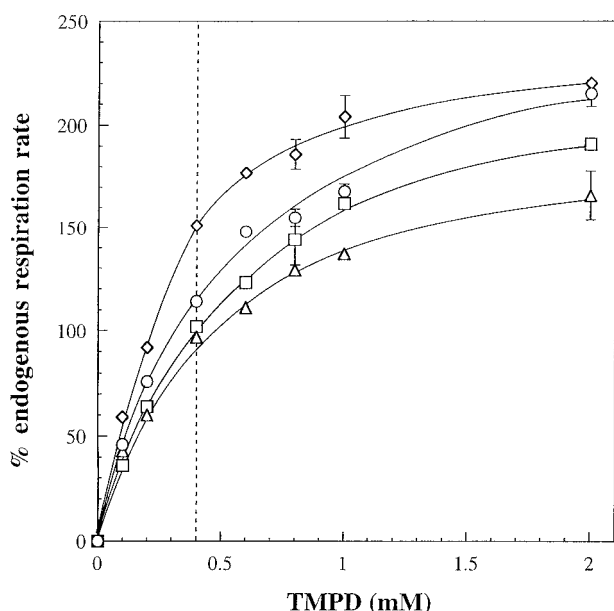
FIG. 3. **Dependence on concentration of TMPD, in the presence of a constant concentration of ascorbate, of the initial O$_2$ consumption rate associated with isolated COX activity in DNP- and antimycin A-treated lung carcinoma cells ($\diamond$), myeloma cells (O), neuroblastoma cells ($\square$) and hepatoma cells ($\triangle$), expressed as a percentage of the uncoupled endogenous respiration rate.** The data shown represent the means $\pm$ S.E. (the *error bars* falling within the symbols are not shown) obtained in 2–4 determinations (one or two independent experiments), utilizing 2.7–4 $\times$ 10^6 cells/ml in the measuring chamber.
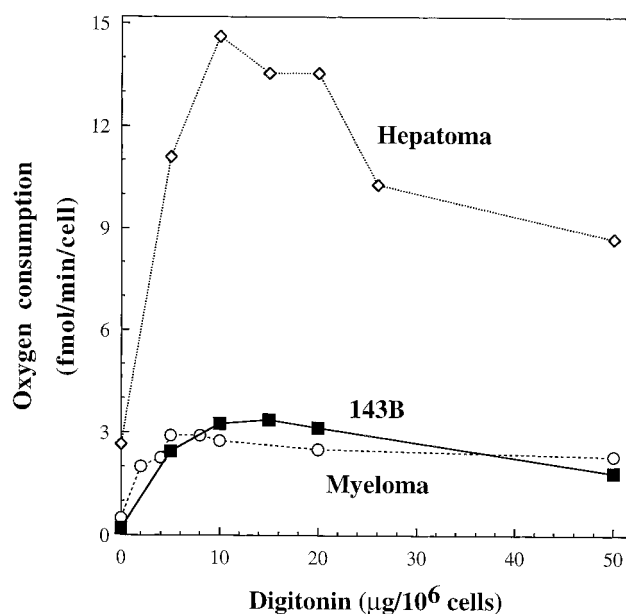

FIG. 4. **Titration of permeabilizing effect of digitonin.** Samples of hepatoma cells (3.3 $\times$ 10^6/ml), 143B.TK$^-$ cells (3.0–3.5 $\times$ 10^6/ml) and myeloma cells (2.7–3.3 $\times$ 10^6 cells/ml) were tested for succinate-dependent respiration in the presence of varying concentrations of digitonin, as detailed under "Experimental Procedures." The data represent the results of single determinations on hepatoma cells or 143B.TK$^-$ cells and of two determinations on myeloma cells.

physiological conditions. Fig. 4 shows the curves illustrating the succinate-supported respiration rate in hepatoma, myeloma, and 143B cells treated with different amounts of digitonin. A digitonin concentration of 15 μg/10^6 cells was chosen as optimal for 143B cells, 10 μg/10^6 cells, for hepatoma cells, and 5 μg/10^6 cells, for myeloma cells. For fibroblasts, a concentration of 10–15 μg/10^6 cells, as recommended by others (15), was adopted. The state 3 (ADP-stimulated) glutamate/malate-dependent respiration rates in digitonin-permeabilized 143B cells, hepatoma cells, myeloma cells, and fibroblasts were found to be very similar to the coupled endogenous respiration rates of intact cells, thus allowing the titration of the same COX activity under different metabolic conditions, but under comparable respiratory fluxes. Fig. 5 presents the threshold plots for 143B, myeloma and hepatoma cells in state 3, showing that the extrapolation of the least-square regression lines through the *filled symbols* beyond the inflection point to zero COX inhibition gives COX$_{R(\mathrm{max})}$ estimates of 1.22, 1.15, and 1.20, respectively. Table II shows the COX$_{R(\mathrm{max})}$ value similarly estimated for fibroblasts. It is clear that the COX$_{R(\mathrm{max})}$ values for state 3 of all cell types analyzed are very similar to the COX$_{R(\mathrm{max})}$ values for the uncoupled state, with a tendency to be somewhat lower (Table II). It has to be stressed, however, that mitochondria (both *in situ* and as isolated organelles) have, in state 3, a residual steady-state transmembrane electrochemical potential (Δp), which continues to exert its back pressure on the electron flow through the whole respiratory chain or the isolated cytochrome *c* oxidase. This has been verified, in our experiments, by the observation of further stimulation of oxygen consumption upon exposure to DNP of state 3-respiring permeabilized cells (data not shown). This residual transmembrane electrochemical potential may account for the observation that the least-square regression lines through the *symbols* beyond the inflection point in the curves of Fig. 5 do not extrapolate to 100% COX inhibition.

DISCUSSION

The fundamental conclusion of this paper is that in a considerable variety of human cell types, COX capacity, measured in intact uncoupled cells or in digitonin-permeabilized cells in state 3, appears to be in low excess or nearly limiting, respectively, relative to the capacity needed to support endogenous or glutamate/malate-dependent respiration. These observations thus extend to a larger range of cell types and to a nearly physiological situation (state 3 respiration) the conclusion, previously suggested by observations on uncoupled 143B cells and related pT3 cells (12), that the *in vivo* control of respiration by cytochrome *c* oxidase is tighter than generally assumed. The commonly held view of the occurrence in mammalian cells of a relatively large excess (2–3-fold) of cytochrome *c* oxidase (7, 9–11, 22) was based on measurements made on isolated mitochondria. However, it has recently been emphasized that the metabolic control analysis of respiration carried out in isolated organelles can be limited by various factors, including the possible loss of metabolites from mitochondria during isolation and the nonphysiological conditions of substrate concentration and delivery. An important additional factor that could influence the functional properties of isolated mitochondria is the loss of interactions with the cytoskeleton (23, 24) and/or other cellular organelles (25). A more physiological situation is attained when mitochondria are analyzed *in situ* in permeabilized systems, such as saponin- or glycerol-skinned muscle fibers (26–28) and digitonin-permeabilized cells (15, 29). For this purpose, we have optimized the digitonin permeabilization conditions so as to obtain respiratory fluxes with NAD$^+$-linked substrates comparable to the coupled endogenous respiration of intact cells. Under these conditions, permeabilized 143B cells and fibroblasts exhibited respiratory control ratios as high as 5–6, very close to the *in vivo* coupling values of oxidative phosphorylation, measured in the same intact cells as ratios of coupled respiration rate to oligomycin-inhibited respiration
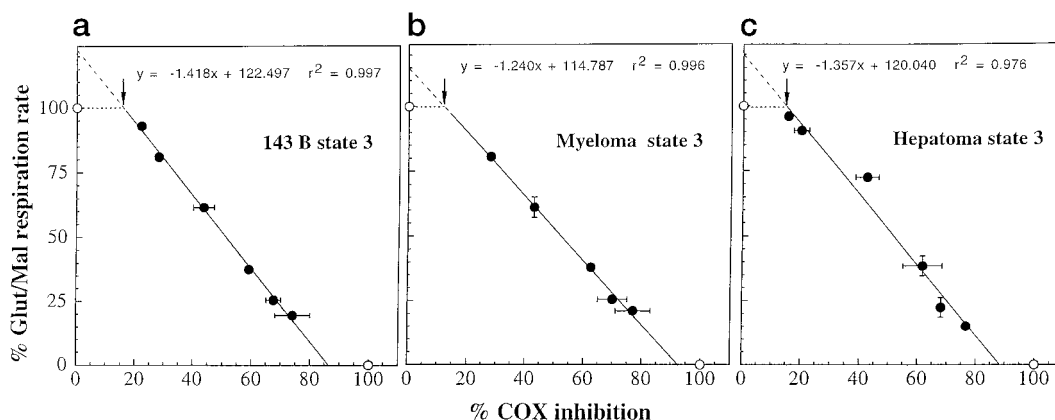
Low Reserve of Cytochrome c Oxidase Capacity in Vivo

FIG. 5. **Percentage of glutamate/malate-dependent respiration rate in digitonin-permeabilized 143B.TK⁻ cells (*a*), myeloma cells (*b*), and hepatoma cells (*c*) as a function of percentage of COX inhibition, with determination of maximum COX capacity (state 3 COX$_{R(max)}$).** The least-square regression line through the *filled symbols* beyond the inflection point in each curve (*arrow*) was extended to zero COX inhibition. The equations describing these extrapolated lines are shown.

rate.[2] In this way, we could titrate COX activity avoiding a possible overestimation of the maximum COX capacity due to upstream inhibition of electron flux (as mimicked in 143B cells partially inhibited with rotenone or antimycin; see Fig. 6 and Ref. 12). The results obtained with permeabilized cells were fully consistent with those obtained with intact cells.

An important relationship of the relative maximum COX capacity is with the COX respiratory threshold (COX$_T$), *i.e.* the percentage of inhibition of isolated COX activity at which a further decrease in enzyme activity has a marked inhibitory effect on the rate of endogenous respiration. The equations describing the extrapolated lines beyond the inflection point in the threshold plots (Fig. 2, *b* and *d*) conform to the general formula:

$$COX_{Ri} = COX_{R(max)}(100 - x) \qquad (Eq. 1)$$

where *x* represents the percentage of inhibition of COX activity at [*i*] (concentration of inhibitor), as detected by KCN titration of the isolation step, and *Ri* represents the endogenous respiration rate at [*i*], expressed as a percentage of the uninhibited endogenous respiration rate. From Equation 1, the threshold value of *x* (COX$_T$) at which COX$_{Ri}$ = uninhibited endogenous respiration rate (100%) (Fig. 2, *b* and *d*) can be calculated according to the following equation:

$$COX_T = 100\left(1 - \frac{1}{COX_{R(max)}}\right) \qquad (Eq. 2)$$

The COX$_T$ values thus determined for the cell types analyzed in the present work, using either intact uncoupled cells or digitonin-permeabilized cells in state 3, are shown in Table II. In previous studies (12), a plot of the COX$_T$ values obtained by Equation 2 from the KCN inhibition data for different cell lines *versus* the independently obtained ratios of oxygen consumption rate supported by 400 μM TMPD in the presence of 10 mM ascorbate (AT400) to uncoupled endogenous respiration rate in the same cell lines, used as estimators of their COX$_{R(max)}$ values, had shown a nearly perfect fit to the curve representing Equation 2. This result had confirmed the reliability of the relative AT400 data for the estimation of COX$_{R(max)}$. Fig. 6*a* shows that the COX$_T$ values and the ratios of AT400 to uncoupled endogenous respiration rate obtained for the cell types analyzed in the present work fit well the same curve. No such good fitting would be possible with values of relative uncoupled respiration rate obtained at TMPD concentrations significantly
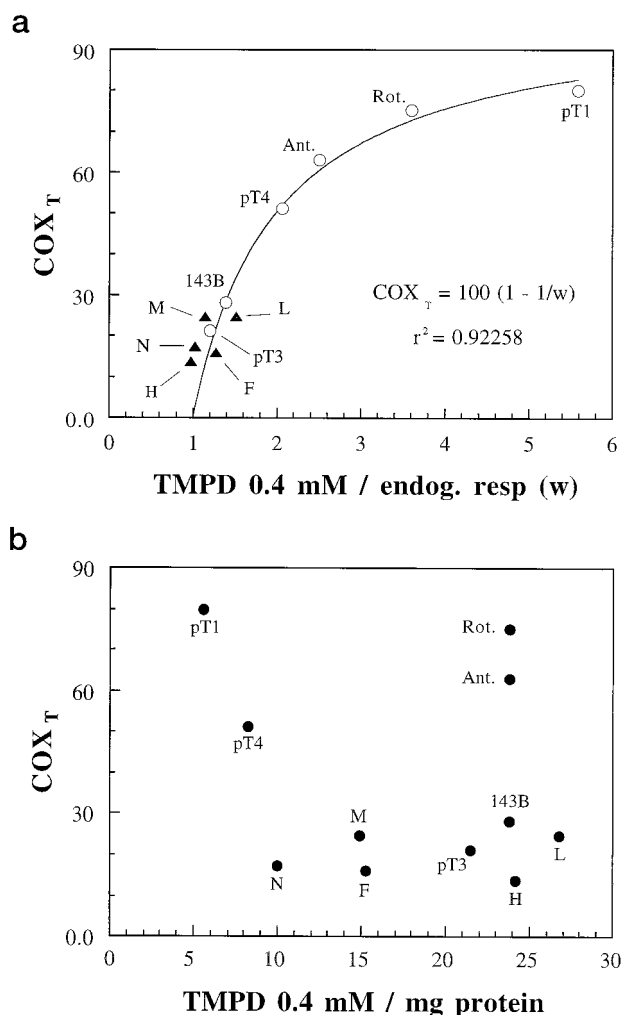

FIG. 6. **Relationship of COX respiratory threshold (COX$_T$) to COX$_{R(max)}$ (*a*) and to cell protein content-normalized COX activity (*b*).** *a*, the data for COX$_T$ obtained in the present work for lung carcinoma cells (*L*), neuroblastoma cells (*N*), myeloma cells (*M*), hepatoma cells (*H*), and fibroblasts (*F*) (▲) and those previously determined (12) for 143B cells, pT3, pT1, and pT4 cells and for 3 nM rotenone- or 2.7 nM antimycin A-treated 143B cells (○) are plotted against the ratios of ascorbate + 0.4 mM TMPD-dependent O₂ consumption rate to endogenous respiration rate, used as estimators of COX$_{R(max)}$. See text for details. *b*, the same data for COX$_T$ are plotted against the values of COX activity promoted by 0.4 mM TMPD, expressed as nmol of O₂/min/mg of protein. For pT3, pT1, and pT4 cells, the same average value of mg of protein/10⁶ cells was used as for the parental 143B cells.

higher than 0.4 mM (data not shown). Particularly significant is the clustering of all the values for the various cell types analyzed in the initial steep portion of the curve (estimated $COX_{R(max)}$ between 1 and 1.5). The fairly large variation in COX_T (14–28%), corresponding to this $COX_{R(max)}$ range, has important implications for the regulatory role of COX in mammalian cell respiration. In fact, it is obvious that in this narrow range of relative COX capacity, any mutation or action of inhibitor or change in physiological conditions that would affect only moderately the activity of COX or of any of the components of the respiratory chain upstream of COX could have a pronounced effect on COX_T and, therefore, on the control of respiration by COX.

The importance of expressing the *in vivo* measurements of COX activity relative to its *in vivo* utilization by the respiratory flux is clearly illustrated by Fig. 6*b*, where the COX_T values are plotted *versus* the COX activity (AT400) expressed relative to total cell protein. In fact, one can see that the scattered distribution of the points does not reveal any relationship between COX activity and the respiratory control exerted by the enzyme in the various cell types.

One can raise the question as to whether the conclusion of the occurrence of a low reserve of COX capacity, as observed in cultured cells, can be extended to tissue cells *in vivo*. It is interesting, in this connection, to compare our results with the similar inhibitor titration analysis of COX activity that was carried out on glycerol-skinned fibers from mouse quadriceps and heart by Kuznetsov *et al.* (26). For this purpose, we have plotted the azide titration data obtained by these authors on permeabilized fibers respiring in state 3 in the presence of glutamate + malate + succinate *versus* the azide titration data of isolated COX activity obtained by the same authors in tissue homogenates. The threshold plots obtained in this way gave $COX_{R(max)}$ values of 1.26 and 1.29 and COX_T values of 22 and 29% for mouse quadriceps and heart fibers, respectively. The same analysis, when applied to the data by Kuznetsov *et al.* (30) on saponin-skinned human muscle (*vastus lateralis*) fibers respiring in state 3 with succinate, using, for the construction of the inhibition curve of the isolated step, a K_D value for azide of 64 μM, as indicated by the same authors, resulted in a $COX_{R(max)}$ value of 1.63 and a COX_T value of 36%. It appears, therefore, that the $COX_{R(max)}$ and COX_T values that can be calculated for fibers from the mouse and human muscles mentioned above from the published data fall in the same range found in the cultured cells analyzed in the present work (Table II and Fig. 6*a*).

Among the factors that have been shown to affect the flux control of COX on respiration in saponin-permeabilized mouse muscle fibers is the oxygen availability within the tissue (31), with a significant increase in flux control having been observed already at an oxygen concentration that is only ~30% lower than the normoxic condition. Therefore, a slightly hypoxic state of the affected muscles could make COX rate-limiting for respiration and, thus, account for the phenotype of mild COX deficiency in muscle observed in several mitochondrial diseases (30, 32, 33), in aging (34) and in COX-deficient mice (26). Similarly, in patients with chronic cardiac ischemia, COX could well become limiting for respiration.

A strong argument can be made that the proposed regulation of COX activity by nucleotides and other allosteric effectors (35–37) would be much more effective if COX were nearly limiting relative to the endogenous respiration, as indicated by the present results. Also, it has been shown that the H^+/e^- stoichiometry of cytochrome c oxidase in rat liver mitochondria (38) or of the purified beef-heart enzyme reconstituted in liposomes (39, 40) varies under the influence of the respiratory

rate. This variation has a possible physiological role in relationship to the dependence of the oxidative phosphorylation efficiency on the rate of electron flux crossing the proton pumps, as shown in yeast mitochondria (41). For the purpose of this kinetic control of the energy conservation properties of COX (which is under the main control of the transmembrane ΔpH), it would be advantageous for the cell to keep the COX capacity within narrow limits of variation with respect to the value at which the enzyme expresses the maximum proton pumping efficiency. In particular, it seems plausible that this value would be close to the level of COX activity required to maintain endogenous respiration in tissues with a fairly constant basal oxidative metabolism, as liver. Liver cells, in fact, exhibited the lowest $COX_{R(max)}$ values among the cell types tested in our work. On the other hand, in tissues with a very high energy demand, which undergo continuous changes in their oxidative metabolism, as is the case for heart and muscle, a higher $COX_{R(max)}$ (as suggested by our relative AT400 data on myoblasts) would be advantageous. In fact, it would allow an adaptation to the variations in oxygen consumption rate in order to keep the enzyme working under the best conditions of energy coupling.

The finding in the present work of a low reserve of COX capacity *in vivo* in the respiratory chain of a variety of human cell types has also relevance to the recently discovered phenomenon of an early release of cytochrome c into the cytosol in cells undergoing apoptosis (42–45). The cytochrome c/cytochrome c oxidase molar ratio, measured in intact cells, has been found to be 1.08 in isolated hepatocytes (46) and 1.62 in rat cardiac myocytes (47). Therefore, the cytochrome c content does not appear to be in large excess over that required for COX activity. Accordingly, a massive loss of cytochrome c, combined with a low $COX_{R(max)}$, in cells undergoing apoptosis may cause a drastic decrease in respiration, with possible mechanistic implications for the execution of programmed cell death.

REFERENCES

1. Kacser, H., and Burns, J. A. (1973) in *Rate Control of Biological Processes* (Davies, D. D., ed) pp. 65–104, Cambridge University Press, Cambridge, United Kingdom
2. Heinrich, R., and Rapoport, T. A. (1974) *Eur. J. Biochem.* **42,** 89–95
3. Groen, A. K., Wanders, R. J. A., Westerhoff, H. V., Van der Meer, R., and Tager, J. M. (1982) *J. Biol. Chem.* **257,** 2754–2757
4. Wallace, D. C. (1992) *Annu. Rev. Biochem.* **61,** 1175–1212
5. Schon, E. A., Bonilla, E., and DiMauro, S. (1997) *J. Bioenerg. Biomembr.* **29,** 131–149
6. Letellier, T., Malgat, M., and Mazat, J.-P. (1993) *Biochim. Biophys. Acta* **1141,** 58–64
7. Letellier, T., Heinrich, R., Malgat, M., and Mazat, J.-P. (1994) *Biochem. J.* **302,** 171–174
8. Taylor, R. W., Birch-Machin, M. A., Bartlett, K., Lowerson, S. A., and Turnbull, D. M. (1994) *J. Biol. Chem.* **269,** 3523–3528
9. Davey, G. P., and Clark, J. B. (1996) *J. Neurochem.* **66,** 1617–1624
10. Davey, G. P., Peuchen, S., and Clark, J. B. (1998) *J. Biol. Chem.* **273,** 12753–12757
11. Davey, G. P., Canevari, L., and Clark, J. B. (1997) *J. Neurochem.* **69,** 2564–2570
12. Villani, G., and Attardi, G. (1997) *Proc. Natl. Acad. Sci. U. S. A.* **94,** 1166–1171
13. King, M. P., and Attardi, G. (1989) *Science* **246,** 500–503
14. Bradford, M. M. (1976) *Anal. Biochem.* **72,** 248–254
15. Kunz, D., Luley, C., Fritz, S., Bohnensack, R., Winkler, K., Kunz, W. S., and Wallesch, C.-W. (1995) *Biochem. Mol. Med.* **54,** 105–111
16. Aden, D. P., Fogel, A., Plotkin, S., Damjanov, I., and Knowles, B. B. (1979) *Nature* **282,** 615–616
17. Lieber, M., Smith, B., Szakal, A., Nelson-Rees, W., and Todaro, G. (1976) *Int. J. Cancer* **17,** 62–70
18. Biedler, J. L., Helson, L., and Spengler, B. A. (1973) *Cancer Res.* **33,** 2643–2652
19. Olsson, L., and Kaplan, H. S. (1980) *Proc. Natl. Acad. Sci. U. S. A.* **77,** 5429–5431
20. Sagi-Eisenberg, R., and Gutman, M. (1979) *Eur. J. Biochem.* **97,** 127–132
21. Brand, M. D., Vallis, B. P. S., and Kesseler, A. (1994) *Eur. J. Biochem.* **226,** 819–829
22. Gnaiger, E., Lassnig, B., Kuznetsov, A., Rieger, G., and Margreiter, R. (1998) *J. Exp. Biol.* **201,** 1129–1139

Low Reserve of Cytochrome c Oxidase Capacity in Vivo

23. Saks, V. A., Kuznetsov, A. V., Khuchua, Z. A., Vasilyeva, E. V., Belikova, J. O., Kesvatera, T., and Tiivel, T. (1995) *J. Mol. Cell Cardiol.* **27,** 625–645
24. Kay, L., Li, Z., Mericskay, M., Olivares, J., Tranqui, L., Fontaine, E., Tiivel, T., Sikk, P., Kaambre, T., Samuel, J.-L., Rappaport, L., Usson, Y., Leverve, X., Paulin, D., and Saks, V. A.(1997) *Biochim. Biophys. Acta* **1322,** 41–59
25. Rizzuto, R., Pinton, P., Carrington, W., Fay, F. S., Fogarty, K. E., Lifshitz, L. M., Tuft, R. A., and Pozzan, T. (1998) *Science* **280,** 1763–1766
26. Kuznetsov, A. V., Clark, J. F., Winkler, K., and Kunz, W. S. (1996) *J. Biol. Chem.* **271,** 283–288
27. Kuznetsov, A. V., Mayboroda, O., Kunz, D., Winkler, K., Schubert, W., and Kunz, W. S. (1998) *J. Cell Biol.* **140,** 1091–1099
28. Kunz, W. S., Kuznetsov, A. V., Schulze, W., Eichhorn, K., Schild, L., Striggow, F., Bohnensack, R., Neuhof, S., Grasshoff, H., Neumann, H. W., and Gellerich, F. N. (1993) *Biochim. Biophys. Acta* **1144,** 46–53
29. Rustin, P., Parfait, B., Chretien, D., Bourgeron, T., Djouadi, F., Bastin, J., Rotig, A., and Munnich, A. (1996) *J. Biol. Chem.* **271,** 14785–14790
30. Kuznetsov, A. V., Winkler, K., Kirches, E., Lins, H., Feistner, H., and Kunz, W. S. (1997) *Biochim. Biophys. Acta* **1360,** 142–150
31. Wiedemann, F. R., and Kunz, W. S. (1998) *FEBS Lett.* **422,** 33–35
32. Shanske, S., Moraes, C. T., Lombes, A., Miranda, A. F., Bonilla, E., Lewis, P., Whelan, M. A., Ellsworth, C. A., and DiMauro, S. (1990) *Neurology* **40,** 24–28
33. Geromel, V., Parfait, B., von Kleist-Retzow, J. C., Chretien, D., Munnich, A., Rotig, A., and Rustin, P. (1997) *Biochem. Biophys. Res. Commun.* **236,** 643–646
34. Müller-Höcker, J. (1992) *Brain. Pathol.* **2,** 149–158
35. Kadenbach, B., Barth, J., Akgun, R., Freund, R., Linder, D., and Possekel, S. (1995) *Biochim. Biophys. Acta* **1271,** 103–109
36. Brown, G. C. (1995) *FEBS Lett.* **369,** 136–139
37. Arnold, S., and Kadenbach, B. (1997) *Eur. J. Biochem.* **249,** 350–354
38. Papa, S., Capitanio, N., Capitanio, G., De Nitto, E., and Minuto, M. (1991) *FEBS Lett.* **288,** 183–186
39. Capitanio, N., Capitanio, G., De Nitto, E., Villani, G., and Papa, S. (1991) *FEBS Lett.* **288,** 179–182
40. Capitanio, N., Capitanio, G., Demarinis, D. A., De Nitto, E., Massari, S., and Papa, S. (1996) *Biochemistry* **35,** 10800–10806
41. Fitton, V., Rigoulet, M., Ouhabi, R., and Guerin, B. (1994) *Biochemistry* **33,** 9692–9698
42. Liu, X., Kim, C. N., Yang, J., Jemmerson, R., and Wang, X. (1996) *Cell* **86,** 147–157
43. Yang, J., Liu, X., Bhalla, K., Kim, C. N., Ibrado, A. M., Cai, J., Peng, T. I., Jones, D. P., and Wang, X. (1997) *Science* **275,** 1129–1132
44. Kluck, R. M., Bossy-Wetzel, E., Green, D. R., and Newmeyer, D. D. (1997) *Science* **275,** 1132–1136
45. Bossy-Wetzel, E., Newmeyer, D. D., and Green, D. R. (1998) *EMBO J.* **17,** 37–49
46. Jones, P. D., Orrenius, S., and Mason, H. S. (1979) *Biochim. Biophys. Acta* **576,** 17–29
47. Kennedy, F. G., and Jones, P. D. (1986) *Am. J. Physiol.* **250,** C374–C383